Antibacterial activity and pore-forming properties of ceratotoxins: a mechanism of action based on the barrel stave model

Yannick Bessin[a], Nathalie Saint[a], Laura Marri[b], Daniela Marchini[c], Gérard Molle[a],*

[a]CBS, UMR 5048 CNRS, UMR 554 INSERM, Université de Montpellier 1, 29 rue de Navacelles, 34090 Montpellier, France
[b]Department of Molecular Biology, University of Siena, I-53100 Siena, Italy
[c]Department of Evolutionary Biology, University of Siena, I-53100 Siena, Italy

Abstract

Ceratotoxins are α-helical cationic peptides isolated from the medfly *Ceratitis capitata*. These amphipathic peptides were found to display strong antibacterial activity and weak hemolytic activity. When reconstituted into planar lipid bilayers, ceratotoxins developed highly asymmetric I/V curves under voltage ramps and formed, in single-channel experiments, well-defined voltage-dependent ion channels according to the barrel stave model. The antibacterial activity and pore-forming properties of these molecules were well correlated. Similar experiments performed with synthesized truncated fragments showed that the C-terminal domain of ceratotoxins is strongly implicated in the formation of helical bundles in the membrane whereas the largely cationic N-terminal region is likely to anchor ceratotoxins on the lipid surface.
© 2004 Elsevier B.V. All rights reserved.

Keywords: Ion channel; α-helical peptide; Lipid bilayer; Conductance

1. Introduction

Linear α-helical peptides are the most abundant class of antimicrobial peptides involved in the first-line defenses of many species [1]. They are strongly amphipathic and render the membrane permeable, resulting in the death of bacteria. Two main mechanisms are involved in membrane perme-abilization in bacteria. In the barrel stave model, peptides associate to form a bundle of α helices embedded in the membrane to form a transmembrane channel [2,3]. In the "carpet-like" model [4–6], peptides bind to the lipid membrane surface until a threshold concentration is reached and α helices associated with lipids then insert into the bilayer to form a toroidal pore, which ultimately disrupts the membrane.

Ceratotoxins (Ctxs)—short linear cationic peptides 29 to 36 residues in length produced by the female reproductive accessory glands of the medfly *Ceratitis capitata* [7–9]—are antibacterial peptides. Ceratotoxin A (CtxA) has been shown to be highly active against Gram-negative and Gram-positive bacteria and to permeabilize the outer and inner membranes of *E. coli* [7,10]. These antimicrobial properties are well correlated with high levels of pore-forming activity [11]. Indeed, macroscopic and single-channel conductances indicate that ceratotoxin A forms voltage-dependent ion channels in planar lipid bilayers according to the barrel stave model. In contrast, pleurocidin, another α-helical cationic peptide (25 residues) [12] with an amino acid sequence 57% similar to that of ceratotoxins (Fig. 1), exerts its antibacterial activity via the carpet-like mechanism, involving the formation of toroidal pores [13].

The large hydrophilic sector of the α-helix of pleurocidin is probably responsible for the formation of toroidal pores in membranes. In contrast, the characteristics of channels in-duced by CtxA suggest that the very amphipathic C-terminal

```
CtxA-1-36:    SIGSALKKALPVAKKIGKIALPIAKAALPVAAGLVG
                 ++      ++  +       +
CtxD-1-36:    SIGTAVKKAVPIAKKVGKVAIPIAKAVLSVVGQLVG
                 ++      ++  +       +
CtxC-1-32:    SLGGVI----SGAKKVAKVAIPIGKAVLPVVAKLVG
                 ++      +       +          +
Pleurocidin:  GWGSFFKKAAHVGKHVGKAALTHYL
```

Fig. 1. Amino acid sequences of Ctx molecules and pleurocidin.

part of the molecule (with a large hydrophobic sector) is embedded in the membrane whereas the very cationic N-terminal part (with five lysines) is bound parallel to the lipid surface [11].

In this study, we tested this hypothesis by synthesizing and purifying three different truncated CtxA molecules, testing their antimicrobial activity and investigating their pore-forming properties. Our results seem to confirm our previous conclusions concerning the role of the C-terminal part of the molecule in the formation of conducting aggregate.

We also synthesized two other ceratotoxins (CtxC and CtxD) and tested them in the same conditions. As for CtxA, our results suggest that the antibacterial activities of these molecules are exerted according to the barrel stave model.

2. Materials and methods

2.1. Reagents, peptides, and bacterial strains

Palmitoyloleoylphosphatidylcholine (POPC), dioleoyl-phosphatidylcholine (DOPE), palmitoyloleoylphosphatidyl-serine (POPS) and diphytanoylphosphatidylcholine (DPhPC) were purchased from Avanti Polar Lipid (Alabaster, AL, USA). Soybean asolectin IV-S was purchased from Sigma.

CtxD1–36, purchased from Multiple Peptide Systems (San Diego CA, USA), was chemically synthesized according to the deduced amino acid sequence of the protein encoded by the *CtxD* gene [9]. CtxA1–36, CtxA1–29, CtxC1–32 and CtxA1–17 have been described elsewhere [7,14]. The CtxA17–36 fragment was purchased from Neosystem (Strasbourg, France).

The following organisms, cultured in LB medium [15], were used in tests of antibacterial activity: *Escherichia coli* LE392, *Klebsiella oxytoca* KD3 (isolated from *C. capitata* [16]), *Enterobacter cloacae* ED8 (isolated from *C. capitata* [16]), *Salmonella typhimurium* ATCC 23853, *Pseudomonas aeruginosa* ATCC 27853, *Staphylococcus aureus* ATCC 25923 and *Bacillus subtilis* ATCC 6633.

2.2. Conductance experiments

In macroscopic and single-channel conductance experiments, virtually solvent-free planar lipid bilayers were formed by the Montal and Mueller technique [17]. The membrane was formed over a 100–150-μm hole in a Teflon film (10-μm thick), pretreated with a 1:40 mixture (v/v) of hexadecane/hexane, separating two half glass-cells. After 2

h, lipid monolayers were spread on top of electrolyte solution (1 M KCl, 10 mM *N*-2-hydroxyethylpiperazine-*N'*-2-etha-nesulfonic acid (HEPES) pH 7.4) in both compartments. Bilayers were formed by lowering and raising the level of electrolyte in one or both sides and monitoring capacitance responses. The concentration of the 7:3 (w/w) POPC/DOPE solution was 1 mg/ml. Voltage was applied through an Ag/AgCl electrode on the *cis*-side. Ceratotoxins and the various fragments were added from stock solutions in MeOH (10^{-6} M). In macroscopic conductance experiments, the doped membranes were subjected to slow voltage ramps (10 mV/s) and transmembrane currents were fed into an amplifier (BBA-01, Eastern Scientific, Rockville, USA). Current–voltage curves were stored on a computer and analyzed with Scope software (Bio-Logic, Claix, France).

In single-channel recordings of Ctx molecules, a solution of DPhPC was used at a concentration of 1 mg/ml. In order to test the role of the charges of lipids, a 7:3:1 (w/w) POPC/DOPE/POPS mixture (1 mg/ml) or an asolectin solution at 5 mg/ml was used in the reconstitution experiments of CtxA. Currents were amplified and potentials were applied simultaneously by a patch-clamp amplifier (RK 300, Bio-Logic). Single-channel currents were monitored using an oscilloscope (TDS 3012, Tektronix, Beaverton, USA) and stored on a CD recorder (DRA 200, Bio-Logic) for off-line analysis. CD data were then analyzed by the Windac32 (http://www.shareit.com) and Biotools (Bio-Logic) programs. All experiments were performed at room temperature. Data were filtered at 1 kHz before digitising at 11.2 kHz for analysis.

2.3. Antibacterial and hemolysis tests

The antibacterial activity of the various Ctxs was assessed by the inhibition zone assay, essentially as described by Faye and Wyatt [18]. Plates (1-mm thick) contained a 0.1% suspension of the bacterial strain (optical density at 600 nm=0.5) in LB plus 0.7% agarose. Samples were applied to wells (2 mm) punched into the plates, which were then incubated overnight at 37 °C. Hemolysis assays were performed as described by Boman et al. [19], using plates (1-mm thickness) containing a mixture of 0.7% agarose, 3.5% BSA and 3% human erythrocytes in 154 mM sodium phosphate, pH 7.3. The plates were incubated overnight at 37 °C. Melittin (Sigma) was used as a control. We applied 0.6 to 240 μg of peptide (in 10 mM sodium phosphate, pH 6.8) in the various assays.

Lethal and hemolytic concentrations were calculated as described by Hultmark et al. [20].

3. Results

We assessed the correlation between antibacterial activity and pore-forming properties by means of macroscopic and single-channel experiments using planar lipid bilayers. We

determined the lethal concentration of Ctxs for the various bacterial strains.

3.1. Ion-channel formation

3.1.1. Macroscopic current measurements

CtxA, CtxC, CtxD and the fragments CtxA1–29, CtxA1–17 and CtxA17–36 were incorporated into PC/PE planar lipid bilayers formed according to the Montal–Mueller technique [17]. Typically, after 30 min (the time required to stabilize the membrane), the bilayer was submitted to repetitive triangular voltage ramps (10 mV/s). All ceratoxins except the CtxA1–17 and CtxA17–36 fragments induced typical alamethicin-like voltage-dependent macroscopic conductance.

As an example, the behavior of CtxD is illustrated in Fig. 2A. Strong asymmetric exponential branches developed above a voltage threshold (Vc), which depended on the peptide concentration in the bath (here the *cis*-side compartment). Unlike alamethicin, but like CtxC (curves not shown) and CtxA [11], CtxD displayed exponential branches in the negative quadrant whereas no current was measured in the positive quadrant unless the membrane was disrupted several times during the experiment.

Macroscopic current measurements with various ceratotoxin concentrations (between 10^{-8} and 1.6×10^{-7} M) were used to estimate concentration dependence by measuring Va—the shift in voltage threshold produced by an e-fold change in bath peptide concentration. The slope of the curve Ln[Ctx] versus Vc was used to obtain this Va value. For
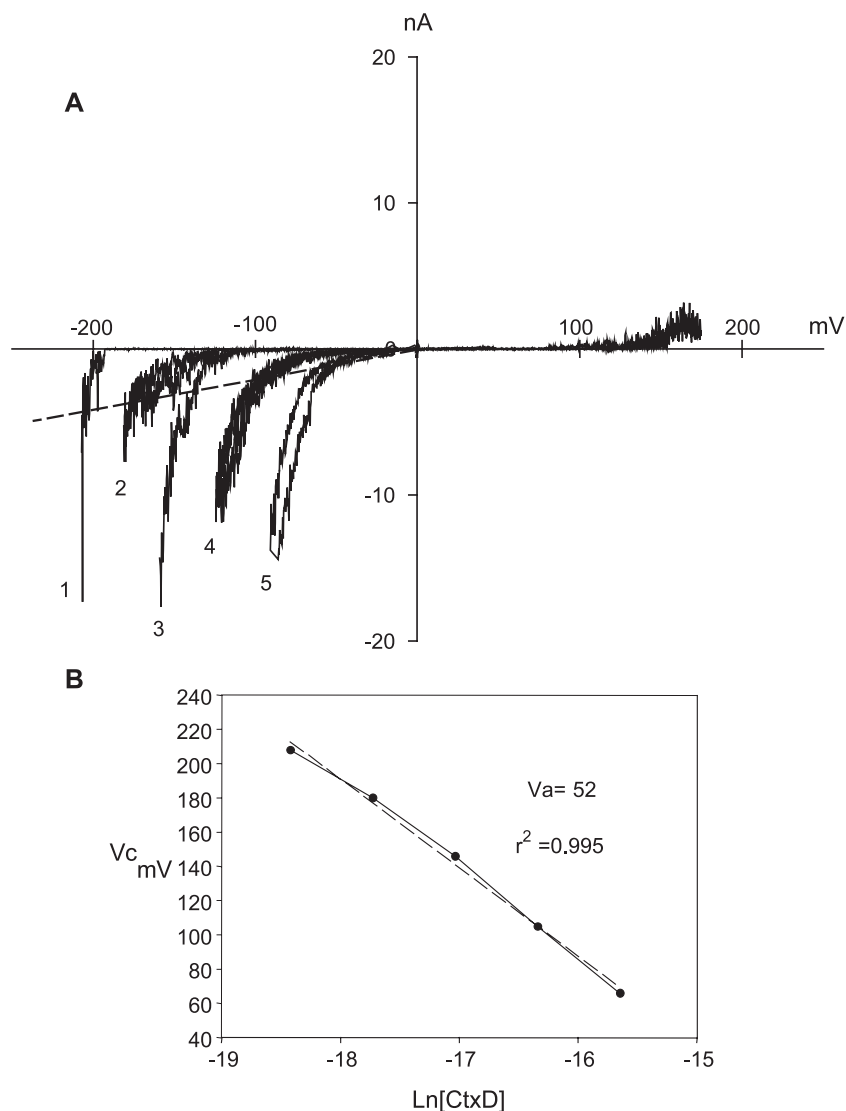

Fig. 2. Macroscopic current–voltage (*I*/*V*) curves of ceratotoxin D at different concentrations in PC/PE membrane and concentration dependence curve. Panel A. *I*/*V* curves between −250 and +250 mV at a ramp sweep of 10 mV/s in 1 M KCl, 10 mM HEPES, pH 7.4, room temperature. Peptide in *cis*-side compartment: curve 1, 10^{-8} M; curve 2, 2×10^{-8} M; curve 3, 4×10^{-8} M; curve 4, 8×10^{-8} M; curve 5, 1.6×10^{-7} M. Panel B. Voltage threshold Vc (determined for a 50-nS conductance, dotted line) was plotted as a function of Ln [peptide concentration]. The slope Va reflects the voltage threshold shift resulting from an e-fold change in bath peptide concentration.

Table 1
Macroscopic conductance parameters for Ctxs

Peptides	Va	Ve	N_{app}
CtxA	50	8.8	5.7±0.5
CtxC	46	13	3.5±0.3
CtxD	52	13.2	4.0±0.3
CtxA1–29	48	12	4.0±0.4

Concentration and voltage dependences, Va and Ve, are given ±3 and ±0.5 mV, respectively.

CtxD, this Va value was about 52 mV, with a high regression coefficient (r^2=0.995) (Fig. 2B) whereas with CtxC, the Va value was 46 mV (r^2=0.992). From these I/V curves, it was also possible to calculate the voltage dependence factor Ve. This value is required to estimate the number of monomers (N_{app}) involved in the formation of the bundle of helices, as N_{app}=Va/Ve. The Ve value is the vol-

tage shift resulting in an e-fold change in conductance. We obtained a Ve value of 13.2 mV for CtxD, giving a N_{app} of about 4. The values obtained for the various ceratotoxins are presented in Table 1. CtxA presented a Ve of 8.8 mV, close to the 6 mV obtained for alamethicin (Alm) [21], indicating a strong voltage dependence, whereas CtxC, CtxD and the truncated CtxA1–29 had Ve values around 13 mV. This difference in behavior also extended to the estimated N_{app} values: around 6 for CtxA versus 4 for CtxA1–29 and CtxD and 3.5 for CtxC. These results suggest that the channel sizes formed with CtxA1–29, CtxC and CtxD are likely to be smaller than that formed with CtxA.

3.1.2. Single-channel experiments

The CtxA1–17 and CtxA17–36 fragments did not induce I/V curves when, in the same range of concentrations used for Ctxs, a doped membrane was subjected to voltage ramps.
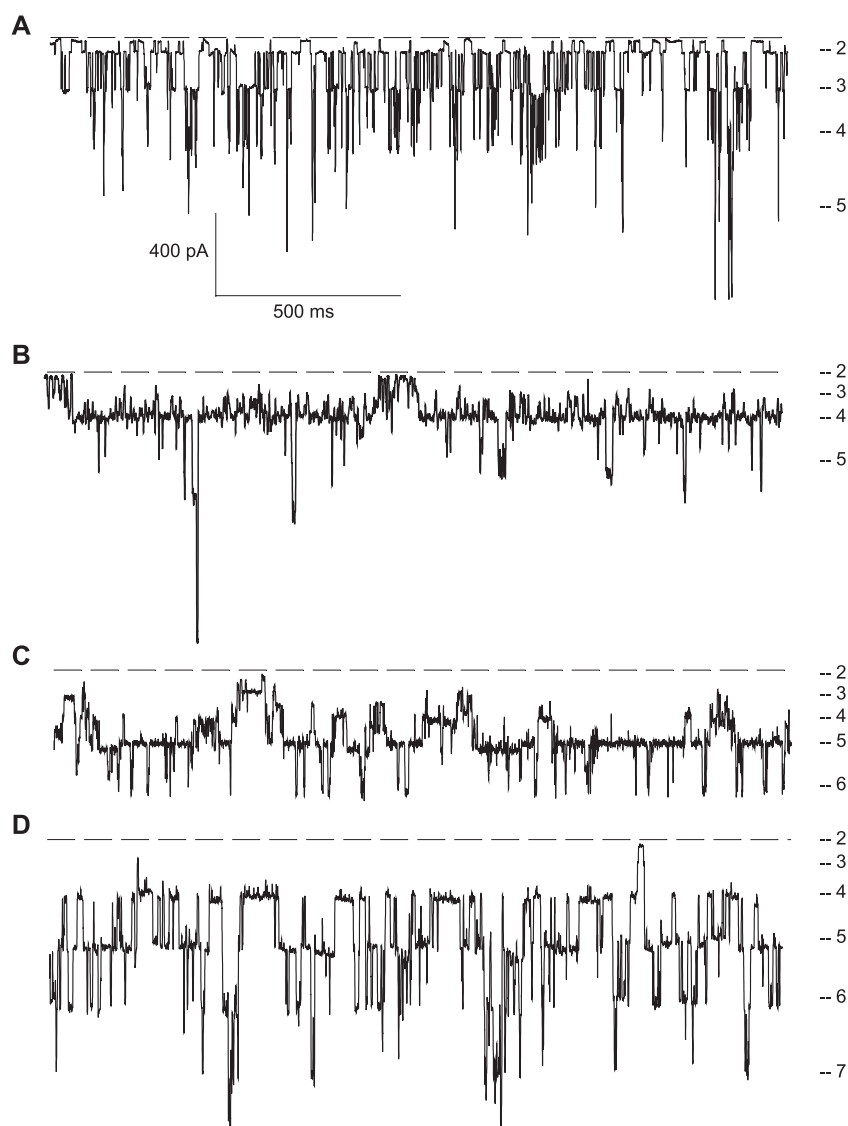

Fig. 3. Single-channel traces for Ctxs in DPhPC bilayers. (A) CtxA, −152 mV; (B) CtxA1–29, −160 mV; (C) CtxC, −158 mV; (D) CtxD, −155 mV. The electrolyte solution was 1 M KCl, 10 mM HEPES, pH 7.4. Peptide concentration was 5×10^{-9} M. The strokes in the right part indicate the various sublevels. The intensity scale does not allow to draw the level 1.

Table 2
Single-channel conductances (in pS) of the substates displayed in DPhPC bilayers by Ctx molecules and by alamethicin [30] in the same conditions and normalized sequences of subconductance ratios*

Substates peptides	1	2	3	4	5	6
CtxA[+174 mV]	80	380	1550	3450	6200	9400
CtxC[+160 mV]	50	230	730	1410	2450	3650
CtxD[+165 mV]	50	210	730	1750	3200	4920
CtxA1–29[+160 mV]	50	250	720	2050	3600	
Alm+140 mV	50	250	1100	2250	3650	5250
R*CtxA	1	4.8	19.3	43	77	117
R*CtxC	1	4.6	14.5	28	49	73
R*CtxD	1	4.2	14.6	35	64	88
R*CtxA1–29	1	5	14.4	41	72	
R*Ala	1	5	22	45	73	105

1 M KCl, 10 mM HEPES, pH 7.4, temperature 25 °C. Applied voltages are in brackets.

Table 3
Conductance values and dwell time of sublevels induced by CtxA into DPhPC, asolectin and PC/PE/PS bilayers

		1	2	3	4	5
Conductance	DPhPC	80	380	1550	3450	6200
(pS)	asolectin	90	430	1720	3800	6400
	PC/PE/PS	95	430	1630	3610	6040
Dwell time	DPhPC	nd	3	3	1.4	1.1
(ms)	asolectin	1	43	25	10	5
	PC/PE/PS	5	17	10	4	2

1 M KCl, 10 mM HEPES, pH 7.4, temperature 25 °C.

This lack of pore formation was confirmed in single-channel experiments because no ion channel was observed in planar DPhPC bilayers, regardless of the peptide concentration used. In contrast, the addition of CtxA, CtxA1–29, CtxC or CtxD into the measurement cell led to the formation of well-defined ion channels (Fig. 3). Nevertheless, the traces obtained with CtxA1–29, CtxC and CtxD displayed noisier events. The various subconductance levels determined from the amplitude histograms (not shown) and reported in Table 2 showed non-integral increments between substates. The conductance values observed for CtxA are higher than those found for the others Ctxs: 80, 380 and 1550 pS against 50, 230 and 730, respectively, for the three fist levels for example. This result agrees with the higher N_{app} value (Table 1) calculated for CtxA. The normalized values of subconductance ratios for the various Ctxs and Alm are similar, showing geometric increments between neighboring substates (Table 2). This characteristic conductance property, together with the macroscopic behavior described above, suggests that ion channel formation occurs according to the barrel stave model. Thus, monomers are taken up and released within the conducting aggregate.

We investigated the possible effect of negatively charged lipids on the positive charges of Ctxs by performing experiments in asolectin and PC/PE/PS (7:3:1) bilayers at various voltages. As CtxA performed best in neutral lipids and it was possible to study the kinetics of channel openings and closures with this molecule, we decided to carry out all subsequent experiments with CtxA only. Well-defined ion channels were formed when CtxA was incorporated into negatively charged bilayers subjected to an applied voltage. For example, Fig. 4 shows the behavior of CtxA at −170 mV in a PC/PE/PS bilayer (Fig. 4A) and in a DPhPC bilayer (Fig. 4B). We used the amplitude histograms (not shown) to calculate the conductance values for each sublevel obtained in asolectin and PC/PE/PS (Table 3) and compared these values with those obtained with DPhPC, a neutral lipid. The
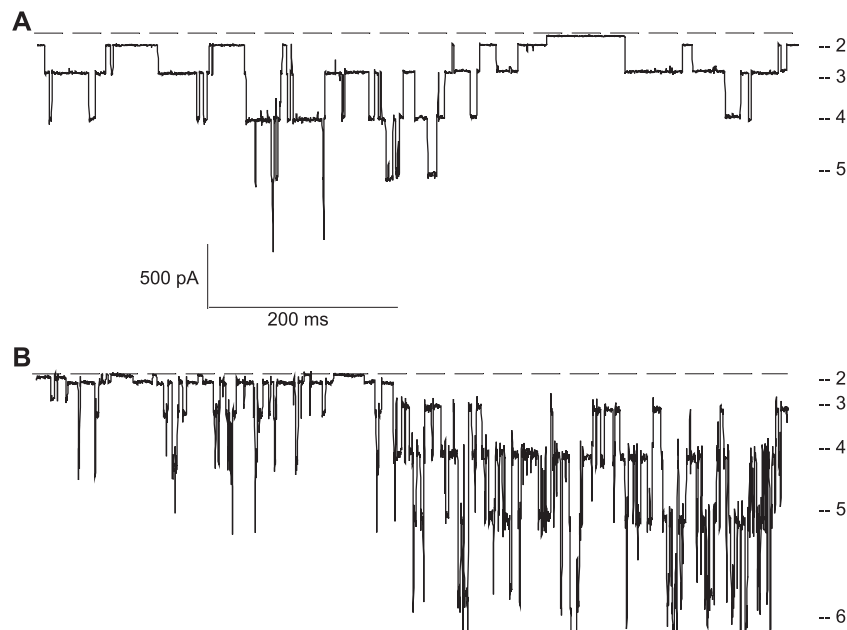

Fig. 4. Single-channel traces induced by CtxA into neutral and charged lipid bilayers. (A) PC/PE/PS; (B) DPhPC. Applied voltage was −170 mV; 1 M KCl, 10 mM HEPES, pH 7.4. Peptide concentration 10^{-8} M. The strokes indicate the different substates. The intensity scale does not allow to draw the level 1.

Table 4
Lethal concentrations and hemolytic activity of Ctx molecules, expressed in μM

Cells	Peptides			
	CtxA	CtxC	CtxD	CtxA1–29
Escherichia coli LE392	1.8	5.7	2.6	5.7
Klebsiella oxytoca KD3*	3.9	21	7.1	5.8
Enterobacter cloacae ED8*	1.7	9.1	7.8	4.5
Salmonella typhimurium ATTC 23853	12	144	38	45
Pseudomonas aeruginosa ATTC 27853	9	174	16	21
Staphylococcus aureus ATTC 25923	95	>350	50	>370
Bacillus subtilis ATTC 6633	1.9	5.3	0.9	6.6
Human erythrocytes	110	645	84	960

An asterisk indicates bacterial strains isolated from *C. capitata* [16].

sublevel conductances obtained for CtxA in the different lipids were similar, indicating that channel size was not modified by the charge on the lipids. The lifetimes of each level were also determined, and were found to differ significantly (Table 3) because channels opened and closed more rapidly in neutral lipids (DPhPC) than in negatively charged lipids (asolectin or PC/PE/PS).

3.1.3. Antibacterial and hemolytic activities of ceratotoxins

The activities of CtxA, CtxA1–29, CtxC and CtxD against several Gram-negative and Gram-positive bacterial strains were found to be in the micromolar range (Table 4). CtxA was the most active peptide, but the values obtained with CtxD were in the same range as those obtained with CtxA. In contrast, the lethal concentrations of CtxC were higher for all the strains used. CtxA1–29 showed a similar activity as that of CtxD against Gram-negative bacteria, whereas it was much less effective against Gram-positives. The values obtained against bacteria isolated from *C. capitata* [16] showed that all four ceratotoxins were efficient against environmental bacteria although CtxA gave the best values: 1.7 μM with *E. cloacae* and 3.9 μM with *K. oxytoca*.

As CtxA1–17 and CtxA17–36 did not form pores, we performed antibacterial tests against *E. coli* LE392 only. With peptide concentrations up to 1000 μM, no antibacterial activity was observed.

Hemolytic tests were performed with human erythrocytes and similar activity was observed for CtxA and CtxD, with values of 110 and 84 μM, respectively. In contrast, CtxC and CtxA1–29, with values of 645 and 960 μM, respectively, presented weaker hemolytic activities.

4. Discussion

Ceratotoxins isolated from the secretions of the reproductive accessory glands of the female medfly *C. capitata* display broad antibacterial activity against Gram-positive

and Gram-negative organisms [10]. Preliminary reconstitution experiments involving the insertion of CtxA into planar lipid bilayers showed that this peptide forms voltage-dependent ion channels according to the barrel stave model. It was suggested that, under an applied voltage, the C-terminal parts of CtxA would associate to form a bundle of five or six monomers whereas the N-terminal moieties, which contain five lysine residues, would bind to the polar heads of lipids [11]. In this study, we investigated the behavior of other ceratotoxins to determine whether the correlation between antimicrobial activity and pore-forming properties observed with CtxA could be generalized to other members of this peptide family. We also synthesized several peptide fragments of CtxA, representative of the N- and C-terminal regions but also the central part. We tested the antimicrobial properties of these molecules and their behavior in reconstitution experiments into planar lipid bilayers, with a view to elucidating their mechanism of action.

CtxA, CtxA1–29, CtxC and CtxD generated similar highly asymmetric I/V curves in PC/PE bilayers, in contrast to CtxA1–17 and CtxA17–36. At various peptide concentrations, they developed exponential branches only in the negative quadrant, indicating preferential insertion in the membrane (see Fig. 2 with CtxD). This result is not surprising given that the N-terminal moieties of CtxA, CtxA1–29, CtxC and CtxD possess three to five positive charges, making it unlikely that this part of the molecule would embed itself within the lipids. In contrast, alamethicin (Alm), the archetype of the barrel stave model, displays strong exponential branches in a positive quadrant [22]. Alm inserts into bilayers via its N-terminal extremity, which is uncharged. However, if the N terminus of Alm is modified to contain one positive charge (NH_3^+ for example; [21]), like the C-terminal parts of Ctx molecules (with one or two lysines), a negative exponential branch is observed. Thus, CtxA1–29, CtxC and CtxD seem to form ion channels via the same mechanism as suggested for CtxA. Nevertheless, the macroscopic conductance characteristics of the various Ctx molecules indicate certain differences (Table 1). Although the values of Va, the concentration dependence factor, were similar in all these molecules, the voltage dependence factor, Ve, was lower for CtxA (8.8 mV) than for CtxA1–29, CtxC and CtxD, which presented values of 12, 13 and 13.2 mV, respectively. Thus, the Va/Ve ratio, which is the apparent number of monomers constituting the bundle of helices in the membrane, was higher for CtxA than for the others Ctxs. It is generally thought that alamethicin exerts its antibacterial activity by membrane permeabilization, and a strong correlation has been found between antibiotic activity and pore size, estimated by N_{app}, the apparent number of monomers constituting the ion channel [23]. Comparison of the lethal concentrations determined for Ctx molecules also demonstrated a strong correlation between this factor and showed also a good correlation with N_{app}. From the Table 4 we see that CtxA

presented the best antibacterial activity in all cases except for *S. aureus* and *B. subtilis* where CtxD is slightly better. In contrast CtxC which presented the lower N_{app} displayed the higher lethal concentration against all organisms. Thus the larger the pore size the lower the minimal inhibitory concentration. The hemolytic activity was also determined for the Ctxs. The values obtained with CtxA and CtxD were about 100 μM, whereas for CtxC and CtxA1–29, we obtained values of 645 μM and 960 μM, respectively. Melittin, a reference cationic peptide, was active at a concentration of 10 μM [24]. Melittin is commonly used to lyse cells and is thought to act against bacteria by inducing "toroidal pores" in zwitterionic membranes and by exerting a detergent-like effect in negatively charged membranes [25]. In this case, the negative charges on the lipids play an important role in the formation of electrostatic interactions with the positive charges of peptides and improve the antimicrobial properties of cationic peptides [26]. The insertion of CtxA into the membrane was not dependent on lipids because single channels presented similar characteristics in neutral and negatively charged bilayers although the kinetics are slower in the charged bilayer than in the neutral one. This finding is consistent with our other results suggesting a barrel stave model for Ctx membrane insertion.

As CtxA1–17 and CtxA17–36 did not form pores, we performed antibacterial tests against *E. coli* LE392 only for these molecules. With peptide concentrations up to 1000 μM, no antibacterial activity was observed (not shown in Table 4). Thus, the N-terminal and C-terminal parts, alone, are not able to induce pore formation in the membrane.

Single-channel experiments confirmed the results already obtained in macroscopic conductance studies and antibacterial tests. When inserted into DPhPC membranes, all the Ctx molecules except CtxA1–17 and CtxA17–36 formed voltage-gated ion channels (Fig. 3). The different subconductance levels with non-integral increments (Table 2) are consistent with the barrel stave model, the fluctuations between substates being correlated with the uptake and release of helical monomers in the bundle [2,3]. The conductance values determined for each level, at similar applied voltages, showed higher conductance sublevels for CtxA than for the other Ctx molecules. This again indicates that CtxA is more active against bacteria than the other molecules tested because, for aggregates comprising the same number of monomers, larger pores were formed with this compound.

We previously suggested [11] that the region corresponding to amino acids 1–17 of CtxA was bound by the positive charges of lysines to the polar head of the lipid whereas, under an applied voltage, the C-terminal part of the molecule would be inserted perpendicularly into the membrane to form the conducting aggregate. Two peptides, CtxA1–17 and CtxA17–36, were synthesized and studied alongside the other Ctx molecules. The lack of activity of CtxA1–17 was expected but we were very surprised to find a similar lack of activity with CtxA17–36, the supposed transmembrane part of CtxA. The well-defined hydrophilic and hydrophobic sectors in the α-helical wheel projection (Fig. 5) of this peptide (with a very narrow hydrophobic section, as for alamethicin) agreed with an eventual membrane activity, although the helical wheel representa-
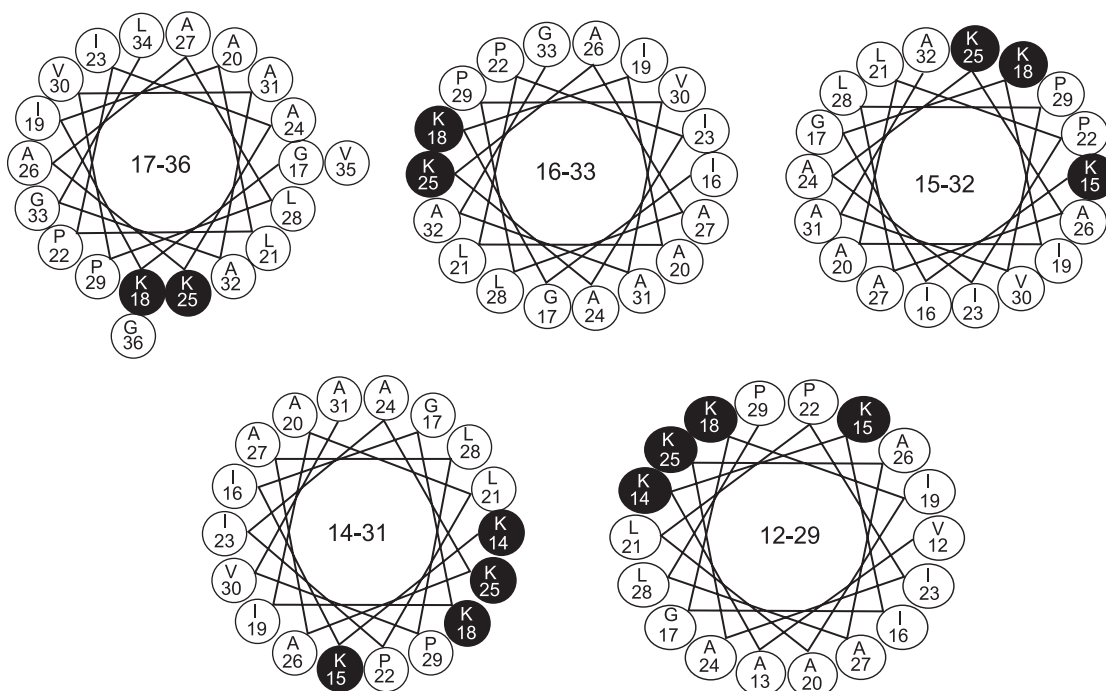

Fig. 5. C-terminal helical wheel projections of CtxA. In black: hydrophilic residues, and in white: hydrophobic residues.

tions do not provide an accurate method to evaluate the potential pore forming activity of CtxA17–36 (due to the presence of both helix breakers Pro22 and Pro29). Similarly, CtxA17–36 was inactive against *E. coli*. It is likely that the two or three residues before Gly$_{17}$ play an important role in the mechanism of action of CtxA. A truncated CtxA1–29 was synthesized and tested successfully in planar lipid bilayers and antibacterial assays. Nevertheless, the observed weaker efficiency of CtxA1–29 in our experiments shows that the presence of residues after Pro$_{29}$ is also important since the longer CtxA displayed the best pore forming properties and antibacterial activities. CD and NMR structural studies showed that CtxA1–30 showed a strong tendency to form α helices in solvent [14] and the topology predictions from databanks predicted a transmembrane helix in the C terminal part. Since CtxA17–36 is inactive and the additional residues after Pro$_{29}$ are necessary, we can suggest that the beginning of the transmembrane helix responsible of the best properties could be located between Lys$_{14}$ and Ile$_{16}$.

The helical wheel projections of these transmembrane parts of CtxA are highly amphipathic, with well-delimited large hydrophobic and small hydrophilic sectors (Fig. 5). The difference of properties between CtxA1–29 and CtxA could be explained by the number of lysines in the hydrophilic sector since we obtain two lysines for CtxA16-33, three lysines for CtxA15–32 and four Lys for CtxA12–29 representing the exact C-terminal part of CtxA1–29 (Fig. 5). In a structural study conducted with lysine-containing amphipathic peptides [27], the authors concluded that polypeptides (LxKy) with a single lysine residue adopted a transmembrane orientation whereas peptides with two separate lysines in the hydrophilic sector were in equilibrium between the plane and the transmembrane orientation. Once more than three lysines were present, the peptides remained preferentially on the surface of the membrane, like pleurocidin, which has four lysines in its hydrophilic sector. Besides, CtxC, which possesses an additional lysine in the hydrophilic sector, displayed the less efficient behavior.

Finally, the substitution of Pro$_{29}$ by Ser$_{29}$ in the hydrophilic sector is probably responsible for slightly lower conductance values and lethal concentrations observed with CtxD. This hypothesis is supported by a study [28] that concluded that the number of bends created by the insertion of proline residues is an important determinant of the antimicrobial, hemolytic and synergistic activity of α-helical peptides.

Yang et al. [4] claimed that only alamethicin behaves in a manner consistent with the barrel stave model and that it is unlikely that antimicrobial peptides with a large number of lysines or arginines permeate the membrane via this mechanism [29]. In this study, we unambiguously showed that cationic peptides such as Ctx molecules can form ion channels via this mechanism. Ceratotoxins present a specific topology, with two well-defined helical parts, one rich in positive charges and the other presenting all the character-

istics necessary for the formation of ion channels according to the barrel stave model. Thus, we suggest that the N-terminal region facilitates the binding of the Ctx molecules to the surface of lipids before the C-terminal part is embedded in the membrane under the applied voltage.

This specific feature may account for the strong correlation between pore-forming properties and antibacterial activity.

Finally, it may be beneficial to use non-peptaibol ceratotoxins—particularly CtxA and CtxD—rather than alamethicin or peptaibols in future biophysical experiments concerning the barrel stave mechanism.

Acknowledgments

References

[1] M. Zasloff, Antimicrobial peptides of multicellular organisms, Nature 415 (2002) 389–395.

[2] G. Baumann, P. Mueller, A molecular model of membrane excitability, J. Supramol. Struct. 2 (1974) 538–557.

[3] G. Boheim, Statistical analysis of alamethicin channels in black lipid membranes, J. Membr. Biol. 19 (1974) 277–303.

[4] L. Yang, T.A. Harroun, T.M. Weiss, L. Ding, H.W. Huang, Barrel-stave model or toroidal model? A case study on melittin pores, Biophys. J. 81 (2001) 1475–1485.

[5] Y. Shai, Mechanism of the binding, insertion and destabilization of phospholipid bilayer membranes by alpha-helical antimicrobial and cell non-selective membrane-lytic peptides, Biochim. Biophys. Acta 1462 (1999) 55–70.

[6] S.J. Ludtke, K. He, W.T. Heller, T.A. Harroun, L. Yang, H.W. Huang, Membrane pores induced by magainin, Biochemistry 35 (1996) 13723–13728.

[7] M. Rosetto, A.G. Manetti, P.C. Giordano, L. Marri, R. Amons, C.T. Baldari, D. Marchini, R. Dallai, Molecular characterization of ceratotoxin C, a novel antibacterial female-specific peptide of the ceratotoxin family from the medfly *Ceratitis capitata*, Eur. J. Biochem. 241 (1996) 330–337.

[8] D. Marchini, P.C. Giordano, R. Amons, L.F. Bernini, R. Dallai, Purification and primary structure of ceratotoxin A and B, two antibacterial peptides from the female reproductive accessory glands of the medfly *Ceratitis capitata* (Insecta:Diptera), Insect Biochem. Mol. Biol. 23 (1993) 591–598.

[9] M. Rosetto, T. De Filippis, A.G. Manetti, D. Marchini, C.T. Baldari, R. Dallai, The genes encoding the antibacterial sex-specific peptides ceratotoxins are clustered in the genome of the medfly *Ceratitis capitata*, Insect Biochem. Mol. Biol. 27 (1997) 1039–1046.

[10] L. Marri, R. Dallai, D. Marchini, The novel antibacterial peptide ceratotoxin A alters permeability of the inner and outer membrane of *Escherichia coli* K-12, Curr. Microbiol. 33 (1996) 40–43.

[11] N. Saint, L. Marri, D. Marchini, G. Molle, The antibacterial peptide ceratotoxin A displays alamethicin-like behavior in lipid bilayers, Peptides 24 (2003) 1779–1784.

[12] A.M. Cole, P. Weis, G. Diamond, Isolation and characterization of pleurocidin, an antimicrobial peptide in the skin secretions of winter flounder, J. Biol. Chem. 272 (1997) 12008–12013.

[13] N. Saint, H. Cadiou, Y. Bessin, G. Molle, Antibacterial peptide pleurocidin forms ion channels in planar lipid bilayers, Biochim. Biophys. Acta 1564 (2002) 359–364.

[14] L. Ragona, H. Molinari, L. Zetta, R. Longhi, D. Marchini, R. Dallai, L.F. Bernini, L. Lozzi, M. Scarselli, N. Niccolai, CD and NMR structural characterization of ceratotoxins, natural peptides with antimicrobial activity, Biopolymers 39 (1996) 653–664.

[15] J. Sambrook, E.F. Fritsch, T. Maniatis, Molecular Cloning: A Laboratory Manual, 2nd ed., Cold Spring Harbor Laboratory, Cold Spring Harbor, NY, 1989.

[16] D. Marchini, M. Rosetto, R. Dallai, L. Marri, Bacteria associated with the oesophageal bulb of the medfly *Ceratitis capitata* (Diptera:Tephritidae), Curr. Microbiol. 44 (2002) 120–124.

[17] M. Montal, P. Mueller, Formation of bimolecular membranes from lipid monolayers and a study of their electrical properties, Proc. Natl. Acad. Sci. U. S. A. 69 (1972) 3561–3566.

[18] I. Faye, G.R. Wyatt, The synthesis of antibacterial proteins in isolated fat body from Cecropia silkmoth pupae, Experientia 36 (1980) 1325–1326.

[19] H.G. Boman, D. Wade, I.A. Boman, B. Wahlin, R.B. Merrifield, Antibacterial and antimalarial properties of peptides that are cecropin-melittin hybrids, FEBS Lett. 259 (1989) 103–106.

[20] D. Hultmark, A. Engstrom, K. Andersson, H. Steiner, H. Bennich, H.G. Boman, Insect immunity. Attacins, a family of antibacterial proteins from *Hyalophora cecropia*, EMBO J. 2 (1983) 571–576.

[21] J.E. Hall, I. Vodyanoy, T.M. Balasubramanian, G.R. Marshall, Alamethicin. A rich model for channel behavior, Biophys. J. 45 (1984) 233–247.

[22] I. Vodyanoy, J.E. Hall, T.M. Balasubramanian, Alamethicin-induced current–voltage curve asymmetry in lipid bilayers, Biophys. J. 42 (1983) 71–82.

[23] H. Duclohier, H. Wroblewski, Voltage-dependent pore formation and antimicrobial activity by alamethicin and analogues, J. Membr. Biol. 184 (2001) 1–12.

[24] T. Unger, Z. Oren, Y. Shai, The effect of cyclization of magainin 2 and melittin analogues on structure, function, and model membrane interactions: implication to their mode of action, Biochemistry 40 (2001) 6388–6397.

[25] N. Papo, Y. Shai, Exploring peptide membrane interaction using surface plasmon resonance: Differentiation between pore formation versus membrane disruption by lytic peptides, Biochemistry 42 (2003) 458–466.

[26] M. Dathe, J. Meyer, M. Beyermann, B. Maul, C. Hoischen, M. Bienert, General aspects of peptide selectivity towards lipid bilayers and cell membranes studied by variation of the structural parameters of amphipathic helical model peptides, Biochim. Biophys. Acta 1558 (2002) 171–186.

[27] B. Vogt, P. Ducarme, S. Schinzel, R. Brasseur, B. Bechinger, The topology of lysine-containing amphipathic peptides in bilayers by circular dichroism, solid-state NMR, and molecular modeling, Biophys. J. 79 (2000) 2644–2656.

[28] L. Zhang, R. Benz, R.E. Hancock, Influence of proline residues on the antibacterial and synergistic activities of alpha-helical peptides, Biochemistry 38 (1999) 8102–8111.

[29] Y. Shai, Z. Oren, From "carpet" mechanism to de-novo designed diastereomeric cell-selective antimicrobial peptides, Peptides 22 (2001) 1629–1641.

[30] O. Helluin, J.Y. Dugast, G. Molle, A.R. Mackie, S. Ladha, H. Duclohier, Lateral diffusion and conductance properties of a fluorescein-labelled alamethicin in planar lipid bilayers, Biochim. Biophys. Acta 1330 (1997) 284–292.